Heat capacity of sodium silicate glasses: comparison of experiments with computer simulations

2002 J. Phys.: Condens. Matter 14 11655

(http://iopscience.iop.org/0953-8984/14/45/309)

INSTITUTE OF PHYSICS PUBLISHING JOURNAL OF PHYSICS: CONDENSED MATTER

J. Phys.: Condens. Matter **14** (2002) 11655–11669 PII: S0953-8984(02)38125-6

Heat capacity of sodium silicate glasses: comparison of experiments with computer simulations

N Zotov

Mineralogisch-Petrologisches Institut, Universität Bonn, Poppelsdorfer Schloss, D-53115 Bonn, Germany

E-mail: nzotov@uni-bonn.de

Received 13 June 2002, in final form 28 August 2002
Published 1 November 2002
Online at stacks.iop.org/JPhysCM/14/11655

Abstract

The vibrational density of states (VDOS) and the heat capacities of amorphous SiO_2 and several $(Na_2O)_x(SiO_2)_{1-x}$, $x = 0.2, 0.333, 0.5$, silicate glasses have been calculated using computer models generated by molecular dynamics and the reverse Monte Carlo method. Significant changes in the VDOS upon addition of Na_2O are predicted. Comparison with experimental data and previous calculations shows that the heat capacity is sensitive mainly to the strength of the Na–O and Si–O pair interactions but not to the medium-range order and the preparation history of the models. It is demonstrated that the increase of the specific heat with increasing alkali oxide for $T > 30$ K is due to an increase of the Na and non-bridging oxygen partial heat capacities.

1. Introduction

Many thermodynamic properties of condensed matter phases (such as heat capacity, vibrational entropy, thermal expansion coefficient, atomic displacements etc) can be calculated if the frequency and temperature dependence of the vibrational density of states (VDOS) is known [1]. While the calculation of the VDOS of crystals using lattice dynamics is well understood, it is not a trivial task in the case of disordered materials (glasses and liquids) due to the lack of long-range order. Therefore, comparison between experimental and calculated heat capacities of glasses can provide important insights on the character of the atomic motions and additional constraints on the VDOS derived from simulations.

The relations between the heat capacity at constant pressure (C_p) at low temperatures and the VDOS of glasses has attracted significant attention because many 'strong' glasses show several low-temperature thermal anomalies [2] (increasing of C_p below 1 K, maximum and plateau in C_p/T^3 at about 10–20 K, plateau in the thermal conductivity at about 10 K). Most of the computational work so far has been done on amorphous SiO_2 (a-SiO_2). Buchenau *et al* [3] have calculated C_p between 5 and 20 K using VDOS extracted from neutron inelastic

scattering data. Taraskin and Elliot [4] as well as Oligschleger [5] have calculated C_v in the range 1–100 K using VDOS, determined from molecular dynamics (MD) simulations. The only calculation of the heat capacity of a-SiO_2 at higher temperatures (up to 1400 K) was reported recently by Horbach *et al* [6]. Stein and Spera [7] have calculated C_v of a-SiO_2 at the glass transition temperature $T_g \sim 1500$ K and at several much higher temperatures ($2500 < T < 4000$ K) in the melt. The characteristic feature of all previous low-temperature C_v calculations is that the calculated C_v/T^3 remains significantly lower than the experimental data and does not reproduce the increase of the experimental C_p/T^3 below 1–2 K. The reasons for these discrepancies are not completely understood. Taraskin and Elliot [4] attributed the poor comparison at low temperatures to deficiencies of the finite-size model not describing properly the long-wavelength vibrations. Some authors [5, 6] have corrected for the finite size of their models by adding the Debye contribution

$$C_v^D/T^3 = (4/5)\pi^4 3pR/\Theta_D^3, \tag{1}$$

where p is the number of atoms in the structural unit (3 for SiO_2), R is the gas constant and Θ_D is the Debye temperature. Even with this correction, their C_v values below 20 K are one to two times smaller than the experimental ones. At higher temperatures ($T > 100$ K) the C_v calculated by Horbach *et al* [6] reproduces relatively well the experimental curve. Their C_v is only about 3 J mol^{-1} K^{-1} lower than the experimental C_p at about 1400 K.

Beyond a-SiO_2 much less computational work has been done even on simple silicate glasses and melts. Stein and Spera [7] have calculated the C_v of liquids in the $NaAlSiO_4$–SiO_2 system using MD in the range 2500–4000 K. On the other hand, several empirical equations have been proposed [8–10] for the calculation of C_p of multicomponent silicate glasses above 300 K as a linear sum of the partial molar heat capacities of the constituent oxides which give excellent agreement (1–2% variations) with experimental heat capacity data above 300 K.

Despite the progress in our understanding of the thermodynamics of silicate glasses there are still several important open questions:

(1) the origin of the discrepancies between calculated and experimental heat capacities, especially at low temperatures, and the effects of anharmonicity;
(2) the small difference between the heat capacities of a-SiO_2 and SiO_2 crystalline phases (quartz, crystoballite) [10] for $T > 80$ K;
(3) the reasons why empirical additive equations give reliable results for C_p of multicomponent glasses despite the differences in the structure of silicate glasses and crystalline oxides;
(4) the microscopic origin of the increase of the heat capacity below 1–2 K [11, 12] upon addition of alkali oxides to a-SiO_2 as well as the increase of the heat capacity with increasing alkali content for all temperatures $T > 30$ K [13];
(5) finally, the reasons why the heat capacity below 20 K is a sensitive function of the thermal history of the glass [2].

In order to understand further some of these questions and especially the role of alkali oxides in the heat capacity of silicate glasses we have calculated the heat capacity in a wide temperature range ($0 < T \leqslant T_g$) of computer models with composition a-SiO_2, $Na_2O{\cdot}4SiO_2$, $Na_2O{\cdot}2SiO_2$ and $Na_2O{\cdot}SiO_2$, which cover the *whole* glass compositional range in the Na_2O–SiO_2 system [14]. Several of the models have been constructed previously by classical MD [15–17]. It is well known that the macroscopic properties (e.g. density, glass transition temperature) of glasses quenched from the melt depend on the cooling rate. Since the time scales of the MD simulations used in the present study (comparable with previous studies) are many orders of magnitude shorter than the ones of a typical laboratory experiment, it follows that the MD glass structures are frozen in at much higher glass transition temperatures and depend on

the cooling rate. Vollmayr *et al* [18] have performed a very detailed study of the cooling-rate effects on MD models of a-SiO_2. A decrease of the macroscopic properties (enthalpy, heat capacity, density, thermal expansion coefficient) was observed with decreasing cooling rate in qualitative agreement with real experiments. However, it was shown that the low-temperature heat capacity (below 100 K) shows only a weak dependence on the cooling rate and the calculated heat capacity even at 1500 K is only 2% smaller than the experimental one. Besides that, it was reported that the cooling-rate dependence of the macroscopic properties is much smaller than that of the microscopic properties (such as radial distribution functions and bond-angle distribution functions). The above-mentioned results clearly indicate that below 1500 K the effects of the cooling rate on the calculated heat capacities of MD models play a minor role and meaningful conclusions from the comparison of experimental and calculated heat capacities could be drawn.

In addition, we have also used the reverse Monte Carlo (RMC) technique [19] to generate directly glass models consistent with a given set of experimental diffraction data *without* quenching from the melt. Results are presented for the $Na_2O{\cdot}4SiO_2$ composition.

Different models were used for several compositions to study the effects of medium-range order and preparation history on the heat capacity. Several models were also *relaxed* with different potential parameters in order to study the effects of the Na–O interactions on the heat capacity.

The paper is organized as follows. Section 2 gives details of the calculation of the VDOS and the heat capacity. Section 3 presents the results for the heat capacity of the different models. Section 4 discusses the results and especially the effects of alkali content. Section 5 gives the conclusions.

2. Calculation procedures

One computer model of a-SiO_2, two computer models of $Na_2O{\cdot}4SiO_2$ (denoted NS4_I and NS4_II, respectively), two computer models of $Na_2O{\cdot}2SiO_2$ (denoted NS2_I and NS2_II) and one computer model of $Na_2O.SiO_2$ (denoted NS1 hereafter) are analysed in the present paper.

The a-SiO_2, NS4_I, NS2_I, NS2_II and the NS1 models were generated previously by *classical* MD. The NS4_II model is generated by the RMC method. It contains 234 atoms (box length 15.21 Å) and is a smaller version of the model described in [20].

The a-SiO_2 model contains 648 atoms (box length 21.41 Å). It was constructed using the potential developed by Vashishta *et al* [21]. The equations of motion were integrated with the Beeman–Alben algorithm and a time step of 0.5 fs. The simulations were carried out at constant particle number, constant volume and constant energy (NVE). The total energy was conserved to better than 1 part in 10^4 over the entire simulation [21].

The NS4_I model contains 585 atoms (average box length 20.00 Å), the NS2_I model contains 602 atoms (average box length 20.0 Å) and the NS1 model contains also 602 atoms (average box length 20.05 Å). These models were constructed using a Born–Higgins-type potential, developed by Feuston and Garofalini [22] with a weak Stillinger–Weber three-body term. The equations of motion were integrated with the Nordsieck–Gear algorithm and time step 1 fs. The MD simulations were carried out at constant pressure and constant particle number.

The NS2_II model contains 1080 atoms (box length 24.42 Å). It was constructed using a Vessal-type potential [23]. The equations of motion were integrated with time step 1 fs. The MD simulations were performed at constant pressure and constant particle number.

Further details of the potentials and the MD simulation procedures are given elsewhere [15–17, 21].

2.1. VDOS calculations

The Si–O and Na–O stretching force constants as well as the O–Si–O and Si–O–Si bending force constants of the Kirkwood-type harmonic potential used in the present study have been previously determined from lattice dynamics calculations on crystalline SiO_2 polymorphs and crystalline sodium metasilicate and adjusted to reproduce the position of the main peaks in the polarized Raman spectra of SiO_2 and NS4 glasses [15].

All computer models were first relaxed with the harmonic potential to minimize the strain energy. The eigenfrequencies and the eigenvectors of the dynamical matrices of the relaxed models were then calculated by *direct* diagonalization using the Householder method [24] and different characteristics of the vibrational modes (depending *explicitly* on the eigenvectors) were analysed. We have used models with a maximum of ∼1100 atoms because these calculations are very computer demanding for systems with more than ∼2000 atoms. For much larger systems, usually only VDOS is determined (see for example [6]) because VDOS can be directly calculated from the MD trajectories as the time Fourier transform of the velocity–velocity autocorrelation function [25]. Oligschleger [5] has shown that the VDOSs of a-SiO_2 models (containing 1944 atoms) calculated both using direct diagonalization and from the velocity–velocity autocorrelation function are practically the same.

In the final VDOS each normal mode is additionally broadened with a Gaussian function with full width at half maximum of 10 cm^{-1} in order to take approximately into account the finite size of the models and disorder not present in the computer generated models.

2.2. Heat capacity calculations

The standard thermodynamic expression for the heat capacity at constant volume, C_v, is given by [1]

$$C_v = -T(\partial^2 F/\partial T^2)|_V = C_v^H + C_v^A \tag{2}$$

where F is the Helmholtz free energy, C_v^H is the harmonic and C_v^A is the leading-term anharmonic contribution to the heat capacity [1], respectively. The temperature dependence of the harmonic contribution (per mole) is given by

$$C_v^H(T) = 3pR\int_0^\infty u^2 \exp(u)/((\exp(u)-1)^2) g(\nu, T)\,\mathrm{d}\nu \tag{3}$$

where p is the number of atoms in the structural unit, R is the gas constant, $u = hc\nu/k_BT$, $g(\nu, T)$ is the VDOS at a given temperature T, h is the Planck constant, c is the speed of light, k_B is the Boltzmann constant and ν is the frequency. The integral in equation (3) was calculated numerically.

The experimentally measured heat capacity at constant pressure, C_p, is related to C_v by the thermodynamic relation (see [1])

$$C_\mathrm{p}(T) = C_v(T) + \alpha^2(T)TB(T)V(T). \tag{4}$$

Combining equations (2) and (4) $C_\mathrm{p}(T)$ can be written as

$$C_\mathrm{p}(T) = C_V^H(T) + \alpha^2(T)T\mathrm{B}(T)V(T) + C_V^A(T) \tag{5}$$

where $\alpha(T)$ is the thermal expansion coefficient, $B(T)$ is the bulk modulus and $V(T)$ is the molar volume at a given temperature. At high temperatures ($k_BT \gg hc\nu$) the anharmonic contribution C_v^A can be approximated [1] by $-A^2T$, where A^2 is a function of the third derivative of the potential. A can be treated [26] as an empirical adjustable parameter in order to improve the agreement at high temperatures between the calculated and experimental heat capacities.

The calculation of C_p from C_v requires knowledge of all parameters (α, B, V and C_v^A) in equation (5) as a function of T. These data are not available in the whole temperature range $0 < T < T_g$ for the Na_2O–SiO_2 glasses. That is why we have compared directly experimental C_p and calculated harmonic C_v^H data. However, the correction $\alpha^2(T)TB(T)V(T)$ has been calculated at several temperatures for all compositions (see section 3.2.1). It is several orders of magnitude smaller than the experimental errors in measured heat capacities. Therefore the neglect of the $\alpha^2(T)T\mathrm{B}(T)V(T)$ correction should not affect the conclusions derived from a comparison between experimental C_p and calculated C_V heat capacities.

In general, the VDOS in equation (3) depends on the temperature. The experimental temperature dependence of the VDOS even for a-SiO_2 is not known. Horbach *et al* [6] have calculated the VDOS of a-SiO_2 at several temperatures (30, 300 and 1050 K) and have observed changes in VDOS with temperature, the effects being strongest for the high-frequency bands at about 32 and 38 THz. These authors note, however, that the heat capacities of a-SiO_2 calculated using both the 30 K and the 300 K VDOSs give practically the same results. Since reliable data for the temperature dependence of the VDOS of the Na_2O–SiO_2 glasses are practically non-existent, we have replaced, similarly to most previous studies, $g(\nu, T)$ in equation (3) by $g(\nu, T_0)$, where T_0 is a reference temperature (equal to 300 K in the present case).

Knowing the eigenvectors of the dynamical matrix, the so-called atomic participation ratios $\mathrm{APR}_\alpha(\nu)$, $\alpha = 1, 2, \ldots, s$, where s is the number of different types of atom in the model, can be calculated [15]. $\mathrm{APR}_\alpha(\nu)$ is equal to unity if only atoms of type α participate in a given normal mode and is equal to zero if, on the contrary, atoms α do not vibrate in this mode. They are defined in such a way that $\Sigma_\alpha \mathrm{APR}_\alpha(\nu) = 1$ for each ν. The atomic participation ratios can be used to calculate the partial VDOS of the different types of atom as

$$g_\alpha(\nu) = \mathrm{APR}_\alpha(\nu) g(\nu). \tag{6}$$

Knowing the partial density of states we can define partial heat capacities for a given type of atom (α) by substituting $g_\alpha(\nu)$ for $g(\nu)$ in equation (3):

$$C_{v\alpha}^H(T) = 3pR \int_0^\infty u^2 \exp(u)/((\exp(u) - 1)^2) g_\alpha(\nu)\, \mathrm{d}\nu. \tag{7}$$

By definition $\Sigma_\alpha C_{v\alpha}^{\mathrm{H}}(T) = C_V^H(T)$ for each temperature.

3. Results

3.1. Vibrational density of states

The calculated VDOSs for the a-SiO_2 model, the two NS4 models and the NS2_I as well as the NS1 model are given in figure 1. The VDOSs are scaled so that $\int_0^{\nu max} g(\nu)\, \mathrm{d}\nu = 1$. The calculated VDOS for the a-SiO_2 model is in relatively good agreement with both inelastic neutron scattering (INS) experiments [27, 28] and with the VDOS derived from of *ab initio* MD simulations [29]. In contrast, the VDOSs of other MD models [4–6, 18, 30], constructed either with the Vashishta-type potential [21] or with the van Beest *et al* potential [31], show inferior agreement with experiment, especially in the low- and mid-frequency (5–28 THz) ranges.

The character of the vibrational modes in a-SiO_2 has been the subject of numerous studies (for a recent review see [32]). Analysis of the character of the vibrations in Na_2O–SiO_2 glasses has been performed in [15, 33]. That is why only the main effects on VDOS by adding alkali oxide to a-SiO_2 will be briefly summarized again. With increasing Na_2O content the intensity of the modes at about 32 THz, arising in a-SiO_2 from anti-symmetric stretching optic-like vibrations of the bridging oxygens (BO) against the Si atoms, decreases and new stretching vibrational modes appear in the vibrational gap of a-SiO_2 (26–29 THz). These new modes

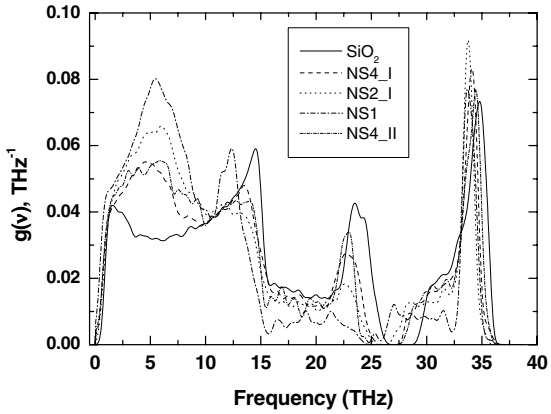

Figure 1. VDOS $g(\nu)$ of the investigated glass models.

are localized on Si–non-bridging oxygen (NBO) atom pairs. The 23 THz band (at about 24 THz in the experimental VDOS [27, 28]) arises from mixed stretching + bending motions of the Si atoms against the BO. The intensity of this band decreases and its position shifts to lower frequencies with increasing Na_2O due to a decrease of the BO concentration. These predictions are in excellent agreement with the only experimental VDOS for alkali silicate glasses ($Li_2O{\cdot}2SiO_2$ glass) measured up to now [28] by INS.

The strong VDOS band at about 15 THz (at about 12–13 THz in the experimental VDOS of a-SiO_2 [27, 28]), arising from symmetric in-plane bending and out-of-plane rocking motion of the Si–O–Si linkages, also decreases in intensity and shifts to lower frequencies. Such changes in the 13 THz band of the $Li_2O{\cdot}2SiO_2$ (LS2) glass were not observed by INS [28]. It is not clear whether this discrepancy indicates some deficiency in our potential model or reflects differences in the structure and the dynamics of the NS2 and LS2 glasses. However, neutron diffraction studies on the LS2 glass (see [28] and references therein) indicate that the average Si–O–Si bond angle is not strongly affected by introduction of Li_2O to a-SiO_2 and thus the 13 THz band should remain mostly unchanged in the LS2 case.

Most dramatic are the changes in VDOS at still lower frequencies, where a new strong band at about 5 THz develops with increasing Na_2O content on top of the underlying bending and rocking SiO_4 modes. Such an effect was not observed in the INS experiments on the LS2 glass [28] simply because the sample contained zero scattering lithium (a mixture of ^{6}Li and ^{7}Li) and thus it did not probe the Li–O dynamics. Analysis of the partial density of states, the atomic participation ratios, the stretching character and the phase quotient (see [15] for detailed description of these vibrational characteristics) indicates that the 5 THz band arises from acoustic-like (bending + stretching)-type motions of the Na atoms mainly against the NBO.

At low frequencies glasses show deviations from the Debye law $g_D(\nu) \sim \nu^2$. In figure 2 we therefore plot $g(\nu)/\nu^2$ for a-SiO_2 and compare with the Debye contribution $g_D(\nu)/\nu^2 = 3/\nu_D^3$. The Debye frequency ν_D and the Debye temperature Θ_D are given by the standard expressions $\nu_D = (3\rho_0/4\pi)^{1/3}v_m$ and $\Theta_D = h\nu_D/k_B$, where ρ_0 is the atom number density and v_m is the average sound velocity. The experimental values of v_m, Θ_D and ν_D for the investigated glasses, where available, are given in table 1.

It can be seen from figure 2 that $g(\nu)/\nu^2$ shows for a-SiO_2 a strong peak at about 1 THz—the so-called boson peak (BP), i.e. an excess VDOS over the Debye value. The shape of the $g(\nu)/\nu^2$ curve is similar to that published in [4], although the position of the BP in this paper is at slightly higher frequency (1.5 THz) and the BP intensity is also higher. For a-SiO_2, Courtens

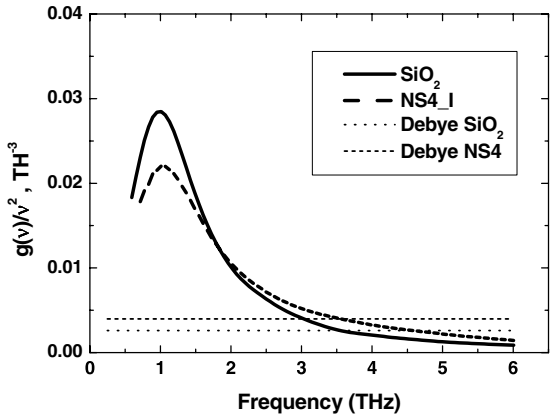

Figure 2. Calculated $g(\nu)/\nu^2$ and the Debye contributions for the a-SIO_2 and NS4_I models.

Table 1. Density ρ_0, sound velocities, Debye temperatures Θ_D and Debye frequencies ν_D for a-SiO_2 and several sodium silicate glasses.

Glass	ρ_0 (atoms Å^{-1})	v_T (km s^{-1})	v_L (km s^{-1})	v_m (km s^{-1})	Θ_D (K)	ν_D (THz)
SiO_2	0.0664	3.77[a]	5.97[b]	4.15	499	10.4
NS4	0.0716[c]	3.2[d]	5.19[d]	3.53	437	9.1
NS2	0.0729[c]	3.15[d]	4.9[d]	3.46	430	8.96

[a] Reference [14].
[b] References [14] and [34].
[c] Reference [35].
[d] Reference [12].

et al [32] have proposed, comparing hyper-Raman and neutron inelastic scattering spectra, that the BP arises from local modes involving rocking motions of distorted SiO_4 tetrahedra. This agrees with an early model proposed in [3].

With the addition of Na_2O the Debye frequencies decrease, due to a decrease in the sound velocities (see table 1), and the Debye contribution $(3/\nu_D^3)$ increases correspondingly. The position of the BP for the NS4_I model practically does not change but the BP intensity decreases. $g(\nu)/\nu^2$ for the NS2 and NS1 models (not given in figure 2) shows no evidence for the presence of a maximum in $g(\nu)/\nu^2$ down to 0.7–1 THz. The lowest frequencies that are accessible from the present models, taking into account the sound velocities given in table 1, are about 1.3–2.0 THz due to the limited system sizes. In order to obtain more reliable results for VDOS below 1 THz it would be necessary to investigate in future much larger models.

3.2. Calculated heat capacities

3.2.1. Amorphous silica. The calculated heat capacity C_v/T^3 for a-SiO_2 in the range 2–100 K is compared with experimental data [36–40] in figure 3(a). The heat capacity C_v up to 1400 K (just below the glass transition temperature $T_g \sim 1500$ K [14, 41]) is shown in figure 3(b). At low temperatures it is useful to compare the heat capacity with the Debye law (equation (1)) and, therefore, to plot at low temperatures C_v/T^3.

The quasi-harmonic correction, $\mathrm{QHC} = \alpha^2(T)TB(T)V(T)$, calculated for two different temperatures (300 and 700 K) is given in table 2. Except for a-SiO_2, experimental data

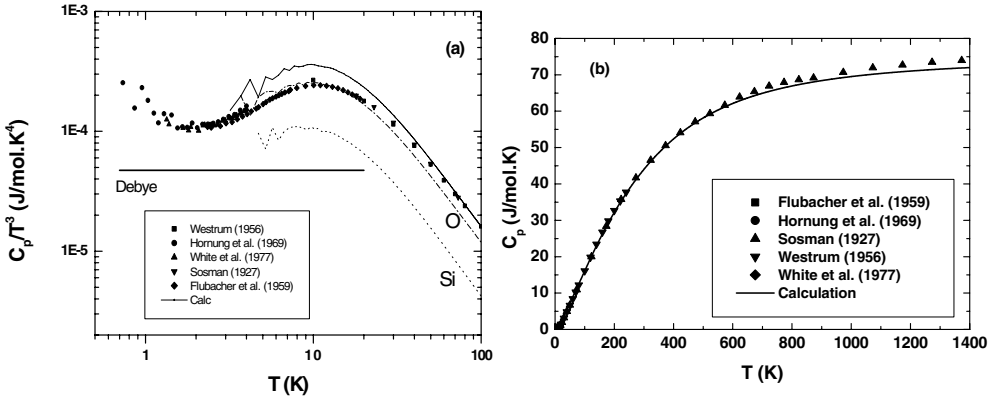

Figure 3. (a) Comparison of experimental $C_{\rm p}/T^3$ (symbols) and calculated heat capacity C_v/T^3 (full curve) for a-SiO_2. The partial heat capacities of O (dash–dot curve) and Si (dashed curve) as well as the experimental Debye level (thick full curve) are also given. Westrum [36], Hornung *et al* [37]; White *et al* [38], Sosman [39]; Flubacher *et al* [40]. (b) Comparison of experimental $C_{\rm p}$ (symbols) and calculated C_v (full curve) for a-SiO_2 up to 1400 K.

for all the parameters—thermal expansion coefficient, bulk modulus and molar volume of the investigated sodium silicate glasses as a function of temperature up to 700 K—are not available. That is why room-temperature values, values for glasses with slightly different composition or values extrapolated from lower temperatures [35, 38, 39, 41–51] have been used for the calculations at 700 K. Despite these uncertainties, the data in table 2 clearly show that the QHCs are one to two orders of magnitude smaller than the experimental errors in $C_{\rm p}$ (typically 1.5–2 J mol^{-1} K^{-1}). Even for NS1 at 700 K the QHC is only about 0.45 J mol^{-1} K^{-1}. This justifies the direct comparison of the calculated C_v with experimental $C_{\rm p}$ data. The changes of QHC with composition will be discussed in section 4.

Figures 3(a) and (b) show that the calculated heat capacity of a-SiO_2 is in good agreement (maximum absolute difference 0.7 J mol^{-1} K^{-1}) with experiments in a wide temperature range from about 20 up to 1200 K. Even below 20 K our data reproduce correctly the plateau at about 10 K and the C_v/T^3 is only about 0.1 log units higher than the experimental values. In previous calculations using MD models generated with different potentials [4–6, 18] the position of the plateau in C_v/T^3 is at higher temperatures ($\sim$20 K) and the calculated heat capacity is significantly lower (for example $\sim$0.5 log units lower at about 10 K and $\sim$1.5 log units lower at about 4 K). Taking into account that the cooling rates in the present and the previous MD simulations of a-SiO_2 [4–6, 18] are similar, the differences in the calculated heat capacities reflect mainly differences in the VDOS (discussed in section 3.1) arising from differences in the interatomic potentials used.

The partial heat capacities of Si and oxygen are also shown in figure 3(a). The partial heat capacities give the first computational proof that at low temperatures the heat capacity of a-SiO_2 is dominated by the oxygen motions as suggested in [3].

3.2.2. Sodium silicate glasses. The calculated heat capacities of the investigated sodium silicate glasses up to 700 K (just below the glass transition temperatures [35]) are shown in figure 4 together with published experimental data [52–56]. The calculated C_v values for all models are in good agreement with the experimental data in a wide temperature range. The temperature T^*, beyond which the difference $\Delta C_{\rm P} = C_{\rm p}^{exp} - C_v^{cal}$ becomes larger than 1–2 J mol^{-1} K^{-1}, decreases with increasing Na_2O content ($T^* \sim 550$ K for NS4, $T^* \sim 400$ K for

Table 2. Thermal expansion coefficient α, bulk modulus B, molar volume V and the QHC to the heat capacity at constant volume for a-SiO_2 and several sodium silicate glasses at selected temperatures. (Standard deviations given in parenthesis.)

	$T = 300$ K				$T = 700$ K			
	$\alpha \times 10^7$ (K^{-1})	$B \times 10^{-6}$ (N cm^{-2})	V (cm^3 mol^{-1})	QHC (J mol^{-1} K^{-1})	$\alpha \times 10^7$ (K^{-1})	$B \times 10^{-6}$ (N cm^{-2})	V (cm^3 mol^{-1})	QHC (J mol^{-1} K^{-1})
SiO_2 [a]	4.5	37	27.3	6.1×10^{-5}	5.5	41	27.3[k]	2.4×10^{-4}
NS4	90[b]	35.2(4)[c]	25.2[d]	2.2×10^{-2}	108[e]	35.2[k]	25.58[d]	7.4×10^{-2}
NS2	142[f]	39.3(1.7)[g]	24.39(5)[i]	5.8×10^{-2}	175[j]	39.3[k]	24.75[l]	2.1×10^{-1}
NS1	194(17)[m]	47.2[n]	23.8[p]	1.3×10^{-1}	237[q]	47.2[k]	24.5[r]	4.5×10^{-1}

[a] The data for a-SiO_2 are taken from [41].
[b] Reference [38].
[c] Average value from [42] and [43].
[d] Reference [35].
[e] Value extrapolated from the data in [44].
[f] Reference [45].
[g] Average value from [42, 45, 46] and [47].
[i] Average value from [39, 48] and [49].
[j] Value extrapolated from data in [50].
[k] Room-temperature value.
[l] Value at $T = 673$ K from [48].
[m] Average value from data in [44] and [51].
[n] Reference [43].
[p] Reference [49].
[q] Value at $T = 658$ K from [44].
[r] Value for $(Na_2O)_{0.45}(SiO_2)_{0.55}$ glass from [35].

NS2 and $T^* \sim 250$ K for NS1). ΔC_p at 700 K is about 4.5–5 J mol^{-1} K^{-1}, which is larger than the typical C_p experimental errors (± 2 J mol^{-1} K^{-1}) and two orders of magnitude larger than the QHCs (see table 2). These results indicate that the anharmonic contributions C_v^A in equation (5) start to play a role in Na_2O–SiO_2 glasses some 200 K below the glass transition temperature.

The difference between the heat capacities of the two NS4 models, relaxed with one and the same set of force constants, is less than 0.5 J mol^{-1} K^{-1} at all temperatures despite the significant *structural* differences between the two models. The NS4_I model is melt quenched while the NS4_II model is generated by the RMC method. This gives further support for the view that the preparation history has a minor effect on the heat capacity. The NS4_II model is more disordered (it has larger Si–O bond-length and bond-angle distortions). The NS4_I model is more polymerized (60.3% Q^4-, 28.2% Q^3- and 7.7% Q^2-species) compared to 38.8% Q^4-, 50% Q^3- and 6.4% Q^2-species in the NS4_II model (where Q^n denotes an SiO_4 tetrahedron with n BO). Evidently, the specific heat of computer generated models calculated in the harmonic approximation is not sensitive to the medium-range order but only to the strength of the Si–O and Na–O pair interactions.

In order to test further these conclusions we have calculated the VDOS and the heat capacity of the NS2_I and NS2_II models using a second set of potential parameters. In the second case the Na–BO and Na–NBO stretching force constants were both equal to 0.6 N m^{-1} instead of 25 and 30 N m^{-1} used initially. The Si–BO–Si bending force constant was also slightly lower (10 N m^{-1}) compared to 14 N m^{-1} used in the first calculation. Both models were first *relaxed* with the *new* set of force constants to minimize the strain energy. The calculated heat capacities of the two models are shown in figure 5. The two NS2 models give practically the same heat capacities despite the fact that they have different medium-range

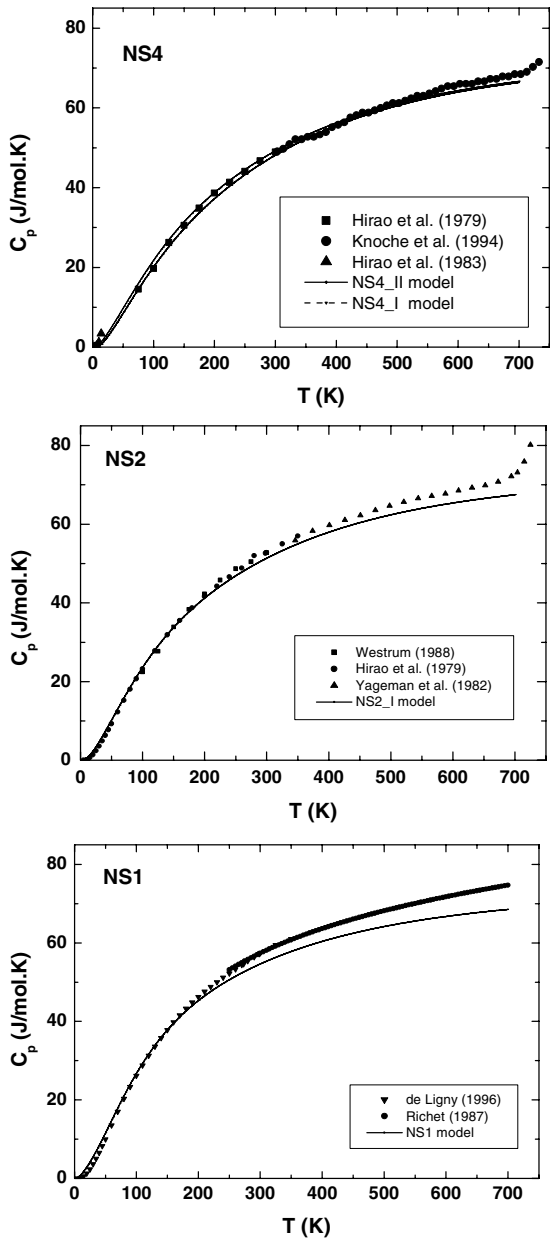

Figure 4. Comparison of experimental C_p (symbols) and calculated heat capacities for several Na_2O–SiO_2 glass models. Hirao *et al* [52]; Knoche *et al* [35]; Hirao *et al* [53]; Westrum [54]; Yageman *et al* [55]; de Ligny [56]; Richet [10].

order and preparation history. Secondly, the agreement between experiment and calculation in the case of *weak* Na–O interactions is very poor below 250 K. These results clearly indicate that the heat capacity is dependent primarily on the strength of the Na–O and Si–O interactions. In addition, they show that the Na–O vibrations dominate the low-temperature heat capacity of Na_2O–SiO_2 glasses.

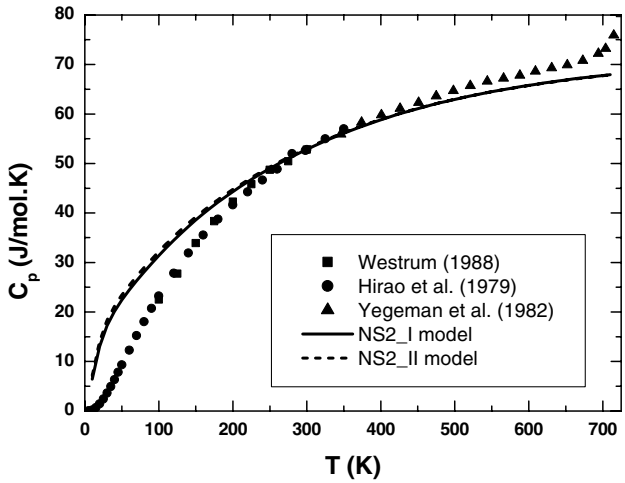

Figure 5. Comparison of experimental C_{p} (symbols) and calculated C_v for the NS2_I model (full curve) and the NS2_II model (dashed curve) relaxed with a second set of force constants. Westrum [54]; Hirao *et al* [52]; Yageman *et al* [55].

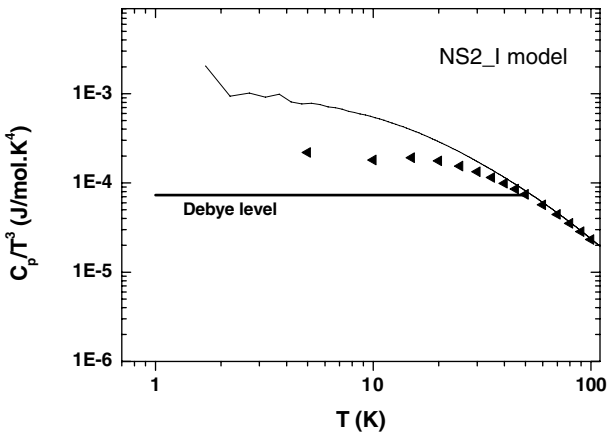

Figure 6. Comparison of experimental C_{p}/T^3 (triangles) and calculated C_v/T^3 (full curve) for the NS2_I model; Debye level—thick full curve.

At low temperatures ($T < 40$ K) C_v/T^3 for the NS2_1 model is about 0.3 log units above the experimental C_{p}/T^3 (figure 6). The results for the NS4 and NS1 models are similar. Both the experimental and the calculated heat capacity data are above the Debye level for $T < 40$ K indicating an excess density of states. Comparison of the partial C_v data (not given in figure 6 for clarity) shows that with increasing Na_2O content the Na and NBO partial heat capacities become larger than the contributions of the Si and BO atoms.

4. Discussion

Heat capacity and INS measurements on permanently *densified* a-SiO_2 have shown that a significant suppression of the VDOS in the range of the BP (0.3–3 THz) and a decrease of the intensity of C_{p}/T^3 in the range 1–100 K is observed upon permanent densification [57]. Neutron diffraction and MD simulations, on the other hand, have shown that the main structural

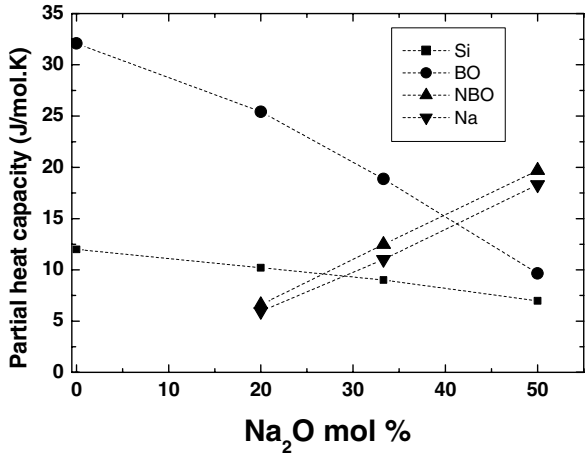

Figure 7. Dependence of the partial heat capacities at $T = 300$ K on the Na_2O content for Si (squares), BO (circles), NBO (triangles) and Na (inverse triangles). The dashed curves are only a guide for the eyes.

effects of the a-SiO_2 densification are a decrease of the average Si–O–Si bond angle and a reduction of the Si–Si correlations. This leads, according to the MD simulations, to an increased frustration in the packing of the SiO_4 tetrahedra [58]. The increased frustration in the packing of the SiO_4 tetrahedra should decrease the local rotational degrees of freedom of the SiO_4 tetrahedra. This could, in turn, qualitatively explain, according to the model proposed in [3] and [32], the observed decrease of the intensity of the BP in densified a-SiO_2.

Such a scenario does not necessarily apply for the Na_2O–SiO_2 glasses. The addition of alkali oxide to a-SiO_2 leads to the formation of NBOs and a more open depolymerized structure. It could be expected that the presence of SiO_4 tetrahedra with several NBOs would enhance the local SiO_4 rocking (rotational) degrees of motion. However, the experimental heat capacities of the investigated Na_2O–SiO_2 glasses decrease in the temperature range 4–30 K. For example, C_p/T^3 for the a-SiO_2, NS2 and NS1 glasses is equal at 10 K to 2.4×10^{-4}, 1.8×10^{-4} and 1.4×10^{-4} J mol^{-1} K^{-4}, respectively [38, 56]. Therefore, the effects of composition on the heat capacity are discussed in more detail below.

The values of the partial heat capacities at $T = 300$ K as a function of the Na_2O content of the models are shown in figure 7. It can be seen that the BO contribution decreases, while the Na and the NBO contributions increase, with increasing Na_2O content. As a result the total heat capacity increases. The behaviour of the partial heat capacities at low temperatures is the same. We have shown that the BO contribution to the heat capacity of a-SiO_2 below 100 K is larger than that of Si (see figure 3(a)). Therefore one probable explanation for the decrease of C_p in the temperature range 5–20 K with increasing Na_2O content could be a decrease of the BO partial heat capacity contribution.

The thermal expansion coefficient α and the calculated QHCs increase by several orders of magnitude with increasing Na_2O content (see table 2). The discrepancy ΔC_p between the heat capacity calculated in the harmonic approximation and the experimental heat capacity at high temperatures (500–700 K) also increases with Na_2O content. In other words, the present data indicate that at high temperatures the anharmonicity of the atomic vibrations increases with alkali content. Anharmonic effects for a given eigenmode could be significant, however, only if the mode is localized [59]. Therefore the localization of the vibrational modes of Na_2O–SiO_2 glasses should increase if the anharmonicity increases as suggested.

The degree of localization is commonly determined by the so-called mode participation ratio $p(\nu)$ [60]

$$p(\nu) = (M_1)^2/(M_0 M_2) \tag{8}$$

where $M_n = \Sigma_\alpha |\boldsymbol{u}_\alpha|^{2n}$ for $n = 0, 1, 2$, α numbers the atoms in the model and $\boldsymbol{u}_\alpha$ is the atomic displacement vector (eigenvector) of atom α vibrating in the normal mode with frequency ν. According to this definition $p(\nu) \to 1$ for delocalized modes and $p \to 0$ for strongly localized modes. Computer simulations have shown [33] that the participation ratio of the vibrational modes of Na_2O–SiO_2 glass models, calculated from equation (8), decreases with increasing Na_2O content. These results support the conclusion that the observed deviations between the experimental heat capacity and that calculated in the harmonic approximation at high temperatures are due to anharmonic effects.

5. Conclusions

We have presented results for the VDOS and the heat capacity of computer generated models of amorphous silica (a-SiO_2) and sodium silicate glasses with 20, 33.3 and 50 mol% Na_2O. The calculated heat capacities are compared to experimental data in a wide temperature range. Calculations of the partial heat capacities are also introduced.

Significant changes in the VDOS of a-SiO_2 upon addition of alkali oxides are predicted, especially the development of a new strong peak at about 5 THz, arising from stretching + bending Na–O interactions.

A good agreement between the experimental and calculated heat capacity of a-SiO_2 is achieved in a wide temperature range (20–1200 K). This result shows that a-SiO_2 is a rather harmonic material thus confirming previous MD analysis [59, 61]

We demonstrate that the discrepancies between the experimental and calculated heat capacities depend mainly on the quality of the interatomic potential used and especially on the strength of the Na–O and Si–O pair interactions.

The heat capacity is not sensitive to the medium-range order of the glass models. This explains the great similarity (for $T > 80$ K) of the heat capacity of a-SiO_2 and SiO_2 crystalline polymorphs as well as the success of the empirical equations for calculation of the heat capacities of multicomponent silicate glasses using the molar heat capacities of the corresponding oxides [8–10]. Namely, despite the fact that the structures of the corresponding oxides (SiO_2, Na_2O, K_2O etc) are quite different from the structure of silicate glasses, the underlying short-range order M–O and Si–O pair interactions are to a great extent the same.

We show that the experimentally observed increase of the heat capacity of alkali silicate glasses with increasing alkali content for $T > 30$ K is due to an increase of the partial heat capacities of Na and the NBO, the concentration of which increases with increasing alkali content. Our results suggest also that the anharmonicity of the atomic vibrations increases with increasing Na_2O content.

Acknowledgments

Part of this work was done with the financial support of the German Science Foundation (project SFB 408). The author thanks Dr W Smith and Dr D Timpel for providing the coordinates of their MD models. The author also thanks Professor P Richet for providing low-temperature heat capacity data for the NS1 and NS2 glasses as well as fruitful comments on an early version of the manuscript.

References

[1] Wallace D C 1976 *Thermodynamics of Crystals* (New York: Wiley)
[2] For reviews, see
Philips W A (ed) 1981 *Amorphous Solids* (Berlin: Springer)
Zeller R C and Pohl R O 1971 *Phys. Rev.* B **4** 2029
Leadbetter A 1975 *J. Phys. Chem. Glasses* **9** 1
Brawer S 1975 *Phys. Chem. Glasses* **16** 2
[3] Buchenau U, Prager M, Nücker N, Dianoux A J, Ahmad N and Phillips W A 1996 *Phys. Rev.* B **34** 5665
[4] Taraskin S N and Elliot S R 1997 *Phys. Rev.* B **56** 8605
[5] Oligschleger C 1999 *Phys. Rev.* B **60** 3182
[6] Horbach J, Kob W and Binder K 1999 *J. Phys. Chem.* B **103** 4104
[7] Stein D J and Spera F J 1996 *Am. Mineral.* **81** 284
[8] Richet P and Bottinga Y 1982 *C. R. Acad. Sci., Paris* **295** 1121
[9] Stebbins J F, Carmichael I S E and Moret L K 1984 *Contrib. Miner. Petrol.* **86** 131
[10] Richet P and Bottinga Y 1986 *Rev. Geophys.* **24** 1
Richet P 1987 *Chem. Geol.* **62** 111
[11] Hunklinger S, Piche L, Lasjaunias J C and Dransfeld K 1975 *J. Phys. C: Solid State Phys.* **8** L423
[12] MacDonald W M, Anderson A C and Schroeder J 1985 *Phys. Rev.* B **31** 1090
[13] Richet P and Bottinga Y 1984 *Geochim. Cosmochim. Acta* **48** 453
[14] Mazurin O V, Sterltsina M V and Shvaiko-Shvaikovskaja T P 1987 *Properties of Glasses and Glass-Forming Liquids* vol 5 (Leningrad: Nauka) p 60 (in Russian)
[15] Zotov N, Ebbsjö I, Timpel D and Keppler H 1999 *Phys. Rev.* B **60** 6383
[16] Timpel D, Scheerschmidt K and Garofalini S-H 1995 *J. Non-Cryst. Solids* **192/193** 267
[17] Smith W, Greaves G N and Gillian M J 1987 *J. Non-Cryst. Solids* **92** 153
[18] Vollmayr K, Kob W and Binder K 1996 *Phys. Rev.* B **54** 15808
[19] McGreevy R L 1995 *Nucl. Instrum. Methods* A **354** 1
[20] Zotov N and Keppler H 1998 *Phys. Chem. Miner.* **25** 259
[21] Vashishta P, Kalia P K, Rino J P and Ebbsjö I 1990 *Phys. Rev.* B **41** 12197
[22] Feuston B P and Garofalini S H 1988 *J. Chem. Phys.* **89** 5818
[23] Vessal B, Amini M, Fincham D and Catlow C R A 1989 *Phil. Mag.* B **60** 753 and references therein
[24] Press W H (ed) 1992 *Numerical Recipes: the Art of Scientific Computing* (Cambridge: Cambridge University Press) ch 11.2
[25] Dickey J M and Paskin A 1969 *Phys. Rev.* **188** 1407
[26] Gillet P 1996 *Phys. Chem. Miner.* **23** 263
[27] Carpenter J M and Price D L 1985 *Phys. Rev. Lett.* **54** 441
Price D L and Carpenter J M 1987 *J. Non-Cryst. Solids* **92** 153
[28] Uhlig H, Bennington S and Suck J B 2000 *J. Phys.: Condens. Matter* **12** 6979
[29] Samthein J, Pasquarello A and Car R 1997 *Science* **275** 1925
[30] Jin W, Vashishta P, Kalia R K and Rino J P 1993 *Phys. Rev.* B **48** 9359
[31] van Beest B W H, Kramer G J and van Santen R A 1990 *Phys. Rev. Lett.* **64** 1955
[32] Courtens P E, Foret M, Hehlen B and Vacher R 2001 *Solid State Commun.* **117** 187
[33] Zotov N 2001 *J. Non-Cryst. Solids* **287** 231
[34] Benassi P, Kirsch M, Masciovechio C, Mazzacurati V, Monaco G, Ruocco G, Sette F and Verbeni R 1996 *Phys. Rev. Lett.* **77** 3835
[35] Knoche R, Dingwell D B, Seifert F A and Webb S L 1994 *Chem. Geol.* **116** 1
[36] Westrum E F Jr 1956 *Trav. IVe Congr Int. Verve (Paris)* 396
[37] Hornung E W, Fischer R A, Brodall G E and Giauque W P 1969 *J. Chem. Phys.* **50** 4878
[38] White G K, Birch J A and Manghnani M H 1977 *J. Non-Cryst. Solids* **23** 99
[39] Sosman R B 1927 *The Properties of Silica (ACS Monographs Series* No 37) (New York: Chemical Catalog) p 856
[40] Flubacher P, Leadnetter A J, Morrison J A and Stoicheff B P 1959 *Phys. Chem. Solids* **12** 54
[41] Bansal N P and Doremus R H 1986 *Handbook of Glass Properties* (Orlando, FL: Academic) p 680
[42] Karapetyan G O, Livshits V Ya and Tennison D G 1981 *Fiz. Khim. Stekla* **7** 188
[43] Manghani M H and Singh B K 1974 *Proc. 10th Int. Congr. on Glass (Kyoto)* vol 11 p 104
[44] Turner W E S and Winks F 1930 *J. Soc. Glass Technol.* **14** 84
[45] Kunugi M, Soga N and Miyashita A 1979 *Rep. Asahi Glass Foundation Ind. Technol.* **35** 79
[46] Appen A A, Kozlovskaya E I and Fuxi Gan Zh 1961 *Prikl. Khim.* **34** 975

[47] Bokin P Ya and Galakhov F Ya 1970 *Neorg. Mater.* **6** 2027
[48] Coenen M 1966 *Glastech. Ber.* **39** 81
[49] Dubrovo S K and Shmidt Yu A 1959 *Zh. Prikl. Khim.* **32** 742
[50] Shermer H P 1956 *J. Res. Natl Bur. Stand.* **57** 97
[51] Shelby J E 1976 *J. Appl. Phys.* **47** 4489
[52] Hirao K, Soga N and Kunugi M 1979 *J. Am. Ceram. Soc.* **62** 11
[53] Hirao K and Soga N 1983 *Rev. Sci. Instrum.* **54** 1583
[54] Westrum E F 1988 Calorimetry in the range 5–300 K *Specific Heat of Solids* ed C Y Ho (New York: Hemisphere)
[55] Yageman V D and Matveev G M 1982 *Fiz. Khim. Stekla* **8** 238
[56] de Ligny D 1996 Proprietes thermiques de mineraux et de silicates vitreaux *PhD Thesis*, Paris
[57] Inamura Y, Arai M, Yamamuro D, Inaba A, Kitamura N, Otomo T, Matsuo T, Bennington S M and Hannon A C 1999 *Physica* B **263/264** 299
[58] Susman S, Volin K J, Price D L, Grimsditch M, Rino J P, Kalia R K and Vashishta P 1991 *Phys. Rev.* B **43** 1194
[59] Taraskin S N and Elliot S R 1999 *Phys. Rev.* B **59** 8572
[60] Bell R J, Dean P and Hibbins-Buttler 1970 *J. Phys. C: Solid State Phys.* **3** 2111
[61] Dell'Anna R, Ruocco G, Sampoli M and Viliani G 1989 *Phys. Rev. Lett.* **80** 1236